

# Prediction of HIV-1 protease resistance using genotypic, phenotypic, and molecular information with artificial neural networks

Huseyin Tunc<sup>1</sup>, Berna Dogan<sup>2</sup>, Büşra Nur Darendeli Kiraz<sup>3,4</sup>, Murat Sari<sup>5</sup>, Serdar Durdagi<sup>6,7</sup>, Seyfullah Kotil<sup>Corresp.</sup>

<sup>1</sup> Department of Biostatistics and Medical Informatics, School of Medicine, Bahcesehir University, Istanbul, Turkey

<sup>2</sup> Department of Medicinal Biochemistry, School of Medicine, Bahcesehir University, Istanbul, Turkey

<sup>3</sup> Department of Biophysics, School of Medicine, Bahcesehir University, Istanbul, Turkey

<sup>4</sup> Department of Bioengineering, Yildiz Technical University, Istanbul, Turkey

<sup>5</sup> Department of Mathematics Engineering, Faculty of Science and Letters, Istanbul Technical University, Istanbul, Turkey

<sup>6</sup> Computational Biology and Molecular Simulations Laboratory, Department of Biophysics, School of Medicine, Bahcesehir University, Istanbul, Turkey

<sup>7</sup> Department of Pharmaceutical Chemistry, School of Pharmacy, Bahcesehir University, Istanbul, Turkey

Corresponding Author: Seyfullah Kotil

Email address: enesseyfullah.kotil@med.bau.edu.tr

Drug resistance is a primary barrier to effective treatments of HIV/AIDS. Calculating quantitative relations between genotype and phenotype observations for each inhibitor with cell-based assays requires time and money-consuming experiments. Machine learning models are good options for tackling these problems by generalizing the available data with suitable linear or nonlinear mappings. The main aim of this paper is to construct drug isolate fold (DIF) change-based artificial neural network (ANN) models for estimating the resistance potential of molecules inhibiting the HIV-1 protease (PR) enzyme. Throughout the study, seven of eight protease inhibitors (PIs) have been included in the training set and the remaining ones in the test set. We have obtained 11803 genotype-phenotype data points for eight PIs from Stanford HIV drug resistance database. Using the leave-one-out (LVO) procedure, eight ANN models have been produced to measure the learning capacity of models from the descriptors of the inhibitors. Mean  $R^2$  value of eight ANN models for unseen inhibitors is 0.732, and the 95% confidence interval (CI) is [0.613,0.850]. Predicting the fold change resistance for hundreds of isolates allowed a robust comparison of drug pairs. These eight models have predicted the drug resistance tendencies of each inhibitor pair with the mean 2D correlation coefficient of 0.933 and 95% CI [0.930,0.938]. A classification problem has been created to predict the ordered relationship of the PIs, and the mean accuracy, sensitivity, specificity, and Matthews correlation coefficient (MCC) values are calculated as 0.954, 0.791, 0.791, and 0.688, respectively. Furthermore, we have created an external test dataset consisting of 51 unique known HIV-1 PR inhibitors

and 87 genotype-phenotype relations. Our developed ANN model has accuracy and area under the curve (AUC) values of 0.749 and 0.818 to predict the ordered relationships of molecules on the same strain for the external dataset. The currently derived ANN models can accurately predict the drug resistance tendencies of PI pairs. This observation could help test new inhibitors with various isolates.

1  
2  
3  
4  
5  
6  
7  
8  
9  
10  
11  
12  
13  
14  
15  
16  
17  
18  
19  
20  
21  
22  
23  
24  
25  
26  
27

**Prediction of HIV-1 protease resistance using genotypic, phenotypic, and molecular information with artificial neural networks**

**Huseyin Tunc<sup>1</sup>, Berna Dogan<sup>2</sup>, Büşra Nur Darendeli Kiraz<sup>3,4</sup>, Murat Sari<sup>5</sup>, Serdar Durdagi<sup>6,7</sup>, Seyfullah Enes Kotil<sup>3,\*</sup>**

<sup>1</sup>Department of Biostatistics and Medical Informatics, School of Medicine, Bahcesehir University, Istanbul, Turkey

<sup>2</sup>Department of Medicinal Biochemistry, Bahcesehir University Medical School, Istanbul, Turkey

<sup>3</sup>Department of Biophysics, School of Medicine, Bahcesehir University, Istanbul, Turkey

<sup>4</sup>Department of Bioengineering, Yildiz Technical University, Istanbul, Turkey

<sup>5</sup>Department of Mathematics Engineering, Faculty of Science and Letters, Istanbul Technical University, Istanbul, Turkey

<sup>6</sup>Computational Biology and Molecular Simulations Laboratory, Department of Biophysics, School of Medicine, Bahcesehir University, Istanbul, Turkey

<sup>7</sup>Department of Pharmaceutical Chemistry, School of Pharmacy, Bahcesehir University, Istanbul, Turkey

\*Corresponding author

[enesseyfullah.kotil@med.bau.edu.tr](mailto:enesseyfullah.kotil@med.bau.edu.tr)

28

29

## 30 Abstract

31 Drug resistance is a primary barrier to effective treatments of HIV/AIDS. Calculating quantitative relations  
32 between genotype and phenotype observations for each inhibitor with cell-based assays requires time and money-  
33 consuming experiments. Machine learning models are good options for tackling these problems by generalizing  
34 the available data with suitable linear or nonlinear mappings. The main aim of this paper is to construct drug  
35 isolate fold (DIF) change-based artificial neural network (ANN) models for estimating the resistance potential  
36 of molecules inhibiting the HIV-1 protease (PR) enzyme. Throughout the study, seven of eight protease inhibitors  
37 (PIs) have been included in the training set and the remaining ones in the test set. We have obtained 11803  
38 genotype-phenotype data points for eight PIs from Stanford HIV drug resistance database. Using the leave-one-  
39 out (LVO) procedure, eight ANN models have been produced to measure the learning capacity of models from  
40 the descriptors of the inhibitors. Mean  $R^2$  value of eight ANN models for unseen inhibitors is 0.732, and the 95%  
41 confidence interval (CI) is [0.613,0.850]. Predicting the fold change resistance for hundreds of isolates allowed  
42 a robust comparison of drug pairs. These eight models have predicted the drug resistance tendencies of each  
43 inhibitor pair with the mean 2D correlation coefficient of 0.933 and 95% CI [0.930,0.938]. A classification  
44 problem has been created to predict the ordered relationship of the PIs, and the mean accuracy, sensitivity,  
45 specificity, and Matthews correlation coefficient (MCC) values are calculated as 0.954, 0.791, 0.791, and 0.688,  
46 respectively. Furthermore, we have created an external test dataset consisting of 51 unique known HIV-1 PR  
47 inhibitors and 87 genotype-phenotype relations. Our developed ANN model has accuracy and area under the  
48 curve (AUC) values of 0.749 and 0.818 to predict the ordered relationships of molecules on the same strain for  
49 the external dataset. The currently derived ANN models can accurately predict the drug resistance tendencies of  
50 PI pairs. This observation could help test new inhibitors with various isolates.

51 **Keywords:** Machine learning; Artificial neural networks; HIV/AIDS; Drug resistance; Protease  
52 inhibitors

## 53 Introduction

54 Acquired immunodeficiency syndrome (AIDS) disease caused by the human immunodeficiency  
55 viruses, HIV-1 and HIV-2, began to spread in the 1970s and came into focus in the early 1980s as  
56 one of the most severe public health threats in history [1]. Detection of reverse transcription

57 activity in cultures of lymph node cells from AIDS patients in the early 1980s revealed that AIDS  
58 was caused by a retrovirus later called human immunodeficiency virus (HIV) [2]. Zidovudine  
59 (AZT), the first nucleotide reverse transcriptase inhibitor (NRTI) that inhibits the reverse  
60 transcription enzyme of HIV, was approved in 1987, and today there are nearly thirty approved  
61 drugs [3]. HIV-1 has affected approximately 38 million people today, and just about 26 million  
62 people are receiving "Highly Active Antiretroviral Treatment" (HAART) [4]. The HAART  
63 therapy proposed in the mid-1990s was defined as the procedure of using three or four different  
64 drugs that act on various targets in the virus's life cycle [5]. With HAART therapy, the death rate  
65 fell to 47% in 1997, just ten years after the first AIDS case was detected [6].

66 Drug resistance is the primary barrier to the effective treatment of HIV/AIDS [7,8]. Single-drug  
67 treatments for HIV yield rapid resistance due to the high genetic diversity and error-prone  
68 replication of the virus [8,9]. Hence, the use of drug combinations through the HAART protocols  
69 increases the efficacy of the treatment [10]. However, cross-resistant isolates for available drugs  
70 encourage researchers to find novel inhibitors [11-15]. To combat drug-resistant isolates, novel  
71 drug design methodologies have been adopted for HIV-1 protease enzyme such as phosphonate-  
72 mediated solvent anchoring [11], lysine sulfonamide-based molecular core [12],  
73 allophenylnorstatine containing inhibitors [13], nonpeptic inhibitor GRL-02031 [14], bis-  
74 tetrahydrofuranylurethane containing nonpeptidic inhibitor UIC-94017 [15]. Testing novel  
75 inhibitors with various drug-resistant isolates need experimental or computational mechanisms.

76 HIV protease enzyme plays a vital role in forming infectious viruses by regulating immature  
77 viruses' synthesized gag and gag-pol polyproteins [16]. Protease inhibitors are generally included  
78 in the scope of HAART therapy, and eight approved drug molecules are used effectively today  
79 [17]. Dose-response curves of protease inhibitors were shown that they have higher Hill coefficient  
80 values than the fusion (FI), integrase (II), nucleoside reverse transcriptase (NRTI), and non-  
81 nucleotide reverse transcriptase (NNRTI) inhibitors [18]. Even if a person is infected with the  
82 wild-type virion, resistant variants may emerge with dosing disruptions or the use of inappropriate  
83 combinations in the HAART therapy [19]. The success rate of HAART therapy can be increased  
84 by measuring the efficacy of existing and novel inhibitors over resistant genotypes [20-21].  
85 Observing drug-efficacy relations with cell-based assays is expensive and time-consuming in the  
86 presence of genotype information. Mathematical models are essential to tackle this important  
87 problem [22-24].

88 Various mathematical models have been calibrated using genotype-phenotype change data  
89 proposed in the Stanford HIV database to predict mutational effects on viral dynamics in the  
90 literature [25-40]. The life span of patients can be considerably extended by constructing reliable  
91 mathematical models that accurately predict suitable drugs for existing isolates. Most existing  
92 prediction models are knowledge-based and require predetermined rules on mutations and drugs  
93 [25-28]. The most commonly used genotype interpretation algorithms have been observed to be  
94 Stanford HIVdb [25], HIV-grade [26], REGA [27], and ANRS [28]. In addition to these genotype  
95 interpretation algorithms, various machine learning models have recently been proposed to predict  
96 genotype-phenotype change relationships in the presence of a predetermined inhibitor [29-40].  
97 Artificial neural network [29-34], random forest algorithm [35-41], support vector machine  
98 [37,41-42], decision trees [43], k-nearest neighbors (kNN) [36], restricted Boltzmann machine  
99 [44], support vector regression [40] and linear regression [45] are the methods used in the literature  
100 to model the efficacy of different drugs against HIV-1 variants. All the works mentioned above  
101 focus on predicting the fold change of mutant fitness under a single drug. Fold change values for  
102 each molecule are treated as disjoint and used to construct a drug-specific model. Those type of  
103 models does not need to take molecular descriptors of a drug as input, hence are indifferent to  
104 chemical structure. Such models cannot predict the effects of resistance mutations for a novel drug.  
105 Therefore, a model that predicts fold change of mutant fitness for multiple molecules is needed.  
106 Here, a machine learning model was constructed that simultaneously takes molecular fingerprints  
107 and mutational information jointly as inputs to estimate the fold change values. For training and  
108 testing sets, we used data from eight approved protease inhibitors atazanavir (AZT), darunavir  
109 (DRV), fosamprenavir (FPV), indinavir (IDV), lopinavir (LPV), nelfinavir (NFV), saquinavir  
110 (SAV) and tipranavir (TPV) in the Stanford HIV drug resistance database. By imposing leave one  
111 out (LVO) test procedure, our drug-isolate-fold (DIF) change-based artificial neural network  
112 (ANN) models are seen to have the ability to learn both from inhibitor descriptors and mutational  
113 genotype information to predict fold-change values. The model can predict the fold change of  
114 hundreds of isolates. To that end, the learned hundreds of predictors (fold-change of isolates) can  
115 be successfully used to assess the resistance potential of inhibitors. We used pairs of drugs to  
116 predict the more resistance-prone molecule. We called these pairwise comparisons the resistance  
117 tendencies. Our DIF-based ANN models predicted each protease inhibitor (PI) pair's drug  
118 resistance tendencies accurately, and these quantitative results support our central arguments.

119

120 **Methods and Material**121 **Dataset Description**

122 Filtered genotype-phenotype data on the Stanford HIV drug resistance database was retrieved for  
 123 PIs [2]. We have organized this dataset with respect to isolates and inhibitors, and 498 protease  
 124 mutations have been observed. For the HIV-1 PI: 1218 isolates for atazanavir (ATV), 678 isolates  
 125 for darunavir (DRV), 1809 isolates for fosemprenavir (FPV), 1860 isolates for indinavir (IDV),  
 126 1562 isolates for lopinavir (LPV), 1907 isolates for nelfinavir (NFV), 1861 isolates for saquinavir  
 127 (SQV) and 908 isolates for tipranavir (TPV) have been analyzed for PI susceptibility. In the  
 128 dataset, 436, 336, 480, 483, 472, 486, 489 and 409 different mutations have been observed for  
 129 ATV, DRV, FPV, IDV, LPV, NFV, SQV, and TPV, respectively.

130

131 **Representation of Isolates**

132 Four hundred ninety-eight unique mutations were observed in the eight protease inhibitors dataset.  
 133 The binary barcoding technique was applied here to represent the isolates that occurred in the  
 134 dataset, as also used in several studies of modeling genotype-phenotype data for various HIV-1  
 135 inhibitors [3]. Thus, a 498-dimensional vector of binary entries with 0s and 1s uniquely  
 136 representing any existing isolates is considered. Assume that the 498 unique mutations produce  
 137 the vector  $X = [x_1, x_2, \dots, x_{498}]$  where  $x_i$  is a mutation pattern that occurred in the dataset. For  
 138 instance,  $x_1$  denotes the occurrence of the mutation A22S or  $x_{478}$  denotes the occurrence of the  
 139 mutation V82A. For example, the isolate  $I_j = [A22S, V82A]$  can be barcoded as  
 140  $X = [1, 0, \dots, 0, 1, 0, \dots, 0]$  in which only the first and four hundred seventy-eighth position take value  
 141 one, and the remaining entries have value zero. Any isolate can be obtained from any combination  
 142 of these mutations, and the isolate  $j$  can be defined as  $I_j = \{a_1, a_2, \dots, a_n\}$  with

$$143 \quad a_k = \begin{cases} 1, & \text{if } x_k \in I_j \\ 0, & \text{otherwise.} \end{cases}$$

144 In this way, each isolate can be transformed into a unique 498-dimensional input vector used for  
 145 the machine learning. The binary barcoding approach has the advantage of representing two or  
 146 more mutational changes in the amino acids since each mutation has a unique position in the 498-  
 147 dimensional input vector. For example, assuming that  $x_{480}$  and  $x_{481}$  denotes mutations V82F and  
 148 V82I, the isolate  $I = [V82F, V82I]$  can be represented as  $X = [0, 0, \dots, 0, 1, 1, 0, \dots, 0]$ . It is important

149 to note that, the genotype-fold change measurements are made on population of viruses, so that it  
150 is possible to find two separate mutations for a single residue.

151

### 152 **Representation of Inhibitors**

153 To construct a drug-isolate-fold change model for the HIV-1 protease inhibitors, the molecular  
154 representations of the inhibitors have been built with binary Morgan fingerprints. The Morgan  
155 fingerprints provide an effective way of the vector representations of molecules and are widely  
156 used in machine learning models [4]. The RDKit environment of the Python program has been  
157 used to convert the smile representations of ATV, DRV, FPV, IDV, LPV, NFV, SQV, and TPV  
158 inhibitors to a binary 512-bit vector representation. 234 out of 512 bits have been seen to provide  
159 unique characteristics for 8 PI. Thus, the molecular representation of each PI needs 234-  
160 dimensional vectors.

161

### 162 **Artificial Neural Network (ANN) Model for Regression**

163 An ANN model has been constructed with isolate-inhibitor inputs and fold change outputs with  
164 the Machine Learning and Deep Learning toolbox of the MATLAB program. Since isolates and  
165 inhibitors are uniquely represented by 498- and 234- dimensional vectors, the ANN model has  
166 732-dimensional input. The ANN architecture includes 732-dimensional input, five hidden layer  
167 neurons, and one output neuron with hyperbolic tangent-sigmoid and linear activation functions.  
168 Logarithms of fold-change values in the dataset are taken as output variables of the neural network  
169 models. In the training process, the scaled conjugate gradient algorithm with MATLAB built-in  
170 function “trainscg” is utilized over GPU [5].

171

### 172 **Ensemble Processing**

173 Since we have only eight inhibitors, measuring the molecular learning capacity of our ANN model  
174 is crucial. In this way, an ensemble learning procedure is used to improve the molecular learning  
175 performance of the model. For each PI, the 100×50 model has been trained with the data of the  
176 remaining seven inhibitors. From every 50 models, a model is chosen that yields the minimum  
177 mean square error for the interior test set of the corresponding PI data. Thus, 100 optimal models  
178 are obtained, and the final model is calculated as the average of these models.

179

## 180 RESULTS

### 181 Regression performance of molecular learning models

182 Eight feed-forward neural network models have been constructed with drug-isolate-fold- change  
183 (DIF) data by excluding one of the drugs from training in each case. The ANN model was trained  
184 with the remaining seven DIF data predicted the excluded results. The sizes of the training and test  
185 sets were changed according to the excluded PIs (mean values are 10328 and 1475 for training and  
186 test sets, respectively). The regression performances of each model are illustrated in Figure 1 with  
187 corresponding  $R^2$  values (square of the linear correlation coefficient). The best and worst results  
188 are obtained by predicting the outcomes of the drugs LPV and TPV with  $R^2 = 0.837$  and  $R^2 =$   
189  $0.393$ , respectively. Similarly, predicting the fold-change results of the inhibitor TPV was  
190 observed to be the worst in the literature [23]. The mean  $R^2$  value of all predictions is  $0.732$  and  
191 the 95% confidence interval is  $[0.613, 0.850]$ . The DIF-based ANN model provides accurate  
192 estimations even if the test data consists of unseen drugs. This observation implies that our ANN  
193 models accurately learn molecular information from the Morgan fingerprints. The detailed  
194 performance results of our DIF-based ANN models are presented in Table 1.

195 An inevitable question is how molecular information changes the regression and classification  
196 performance of our ANN models. To clarify this, we trained isolate-fold-change (IF) based ANN  
197 models for each inhibitor and compared them with the current DIF-based models. In Figures S1-  
198 S2, the model performances have been compared by measuring  $R^2$  and area under the curve (AUC)  
199 values for each PI. Table S1 also shows the accuracy, sensitivity, specificity, and Matthews  
200 correlation coefficient (MCC) scores of both DIF-based and IF-based models. These findings  
201 suggest that the DIF-based ANN model performs slightly better in terms of regression and  
202 classification for six of the eight PIs. The two models are compatible with the remaining two  
203 inhibitors (DRV and TPV). Therefore, the molecular information used by the DIF-based model  
204 provides a better predictive capability. It is very important to note that IF-based models can never  
205 predict fold-change values for novel molecules. The real distinction between DIF and IF-based  
206 models is that the DIF-based model can predict fold-change values for a novel drug. Hence, the  
207 DIF-based ANN model has both better learning capability from mutant information (by comparing  
208 to the IF-based model) and the ability to test novel molecules for a given isolate.

209

### 210 Prediction of drug resistance tendencies for each PI pair

211 The inhibition potential of each PI in the presence of various genotypes is known to be variable.  
212 Tendencies of the logarithmic fold change values for each PI pair provide valuable information  
213 about the resistance profiles of the inhibitors, as seen in Figure 2. Prediction of these tendencies  
214 by the DIF-based ANN models and the corresponding 2D correlation coefficients are presented in  
215 Figure 2 in a comparative way for each PI pair. For each PI, prediction has been made with the  
216 ANN model trained by the data of the remaining seven inhibitors with an ensemble learning  
217 approach. This procedure shows the molecular learning capacity of our ANN models from the  
218 Morgan fingerprints. The minimum and maximum 2D correlation coefficients are 0.892 and 0.954  
219 for TPV-DRV and LPV-DRV couples (95% CI [0.930, 0.938]), respectively. Thus, the current  
220 DIF-based ANN models can distinguish the inhibitory potentials of each PI pair.

221

### 222 **Classification of PIs with respect to possible common isolates**

223 Our DIF-based ANN models can distinguish the fold change values of each PI in the presence of  
224 any isolate. In this way, a classification problem measuring the relationship  
225  $\log(\text{Fold Change } [A, \text{Isolate}]) > \log(\text{Fold Change } [B, \text{Isolate}])$  has been constructed, where  
226 A and B are possible protease inhibitors. These relations take values 0 and 1 depending on the  
227 inhibitors and isolates. Therefore, our ANN models have been trained with the data from seven  
228 inhibitors, with the exception of one particular inhibitor considered as test data. The corresponding  
229 receiver operating characteristic (ROC) curves are illustrated in Figure 3. Area under the ROC  
230 curve (AUC) values are included in the figure. The best and worst AUC values have been obtained  
231 for the IDV-LPV and DRV-LPV pairs with 0.992 and 0.818 (95% CI: [0.950, 0.978]),  
232 respectively. In this context, the current DIF-based ANN models have ability to capture the binary  
233 relations between any PI pair with high approximation performance.

234 Performance metrics of the current ANN models for capturing binary relations of PI pairs are  
235 presented in Table 2. As indicated in the table, the DIF-based ANN models have a high rate of true  
236 prediction for each PI pair. The mean accuracy, sensitivity, specificity and Matthews correlation  
237 coefficient (MCC) values have been computed as 0.954, 0.791, 0.791 and 0.688 (95% CI [0.932,  
238 0.952], [0.719, 0.863], [0.719, 0.863] and [0.600, 0.776]), respectively. The most conspicuous  
239 result here is that the neural network models can classify the inhibitors for resistance profiles, even  
240 if that model did not see the corresponding inhibitors in the training process.

241

## 242 **Testing the molecular learning model with the external data set**

243 For the external dataset, we conducted a search for compounds that were comparable to the eight  
244 HIV PIs that were already available in the ChEMBL database [46]. An initial set of 1305  
245 compounds and their biological activity values were extracted. First, compounds having 70% or  
246 less similarity to each drug were filtered out. Then, molecules with determined  $IC_{50}$  values in  
247 mutant viruses were collected. The compounds with determined  $IC_{50}$  values in mutant viruses  
248 were then gathered. Furthermore, the maximum Tanimoto similarities of these molecules to the  
249 current eight PIs were computed (using 512-bit Morgan fingerprints), and molecules with 40% or  
250 less structural similarity were filtered out. Finally, molecules with 1s in the discarded 278-  
251 dimensional fingerprint vectors, that is, molecules with information loss, were filtered out. A final  
252 dataset of 87 genotype-phenotype relationships involving 51 different molecules was obtained (see  
253 Supplemental Data S1). Only six of these molecules are in the existing PI set (DRV, IDV, NFV,  
254 ATV, LPV) and only 20 of 87 genotype-phenotype relations belong to these six PIs. In the presence  
255 of eight distinct strains, there is a fold change difference in  $IC_{50}$  values for these molecules.  
256 Fortunately, the data includes different molecules tested on the same protein, so we can evaluate  
257 the efficiency of our ANN model on ranking of these molecules.

258 We have used the eight existing PIs (see Figure 4 for chemical structures) to construct an ANN  
259 model as described in the *Methods and Material* section. The main difference is the consideration  
260 of all molecules rather than the LVO procedure. The Morgan fingerprints of the new 51 molecules  
261 were determined, and then the similar mapping was used to reduce the 512-dimensional vectors  
262 into 234-dimensional inputs. It should be noted that the molecules were chosen in such a way that  
263 there are no 1s in the discarded 278 bits. This condition was specifically designed into the external  
264 dataset. In this approach, we ensure that no meaningful information for novel molecules is lost  
265 during the machine learning process.

266 Two different classification performances of our ANN model were observed to test its molecular  
267 learning potential. The first is the classification of resistant and susceptible strains for a given PI,  
268 with a threshold fold change value of 3 [36]. The goal of this classification task is to evaluate the  
269 resistance labeling performance of the current model for diverse molecules. As demonstrated in  
270 Table 3, the accuracy, sensitivity, specificity, MCC, and AUC metrics of our model for labeling  
271 the resistance in external data are 0.678, 0.536, 0.935, 0.468, and 0.843, respectively. Our ANN  
272 model performs satisfactorily statistically on the external dataset as a result.

273 Our major point is that the built ANN model is capable of ranking the efficiency of PIs for a given  
274 strain. The external dataset contains 853 pair of resistance scores for 51 different molecules. Our  
275 ANN model predicted these 853 pair of resistance scores as well, and we measured the ranking  
276 performance of the model. This testing approach is identical to the previously described tendency  
277 and ranking assessments of the eight existing PIs. For this classification task, the accuracy,  
278 sensitivity, specificity, MCC, and AUC scores have been 0.749, 0.767, 0.730, 0.497, and 0.819,  
279 respectively (see Table 3). As a result, our ANN model appropriately ranks the compounds based  
280 on their resistance profiles (see Figure 5 for a representative example). The ROCs for both  
281 resistance classification and ranking classification performances of the ANN model can be seen in  
282 Figure 6. The ANN model learned considerable information from the molecular structure of the  
283 eight PIs, according to the ROCs. In summary, if the external PIs have no information loss (no 1s  
284 in the discarded 278 bits within 512 bits) in comparison to the existing eight PIs, our ANN model  
285 has a high ability to rank these PIs.

286 One method for reducing and visualizing high-dimensional data is principal component analysis  
287 (PCA). It is widely used to describe the chemical space occupied by a set of molecules. When the  
288 descriptors of the compounds are used for analysis, it allows for the clustering of similar molecules  
289 as well as the distinguishing of diverse molecules. To verify the applicability of our model in terms  
290 of chemical similarity and diversity, we have performed the PCA on the external set molecules  
291 using 234-dimensional vectors employed for fold-change prediction. We only evaluated the  
292 unique molecules in the external set, and for molecules that were tested in several strains and had  
293 multiple fold-change prediction values, we have taken the values with the largest absolute  
294 prediction error (AE). As the first two components, PC1 and PC2, were able to represent more  
295 than half of the variance in the data and accurately depict the correlations between the similarities  
296 of the molecules, 234-dimensional vectors for each unique molecule were projected to 2D-space.  
297 Figure 7 displays the PCA plot for both training and external set compounds and colored according  
298 to the AE for fold-change prediction or training compound name. According to the figure, other  
299 training compounds other than the IDV were not involved in cluster formation with external set  
300 molecules. Though the same external set molecules were not forming clusters, still there were three  
301 clusters that contain three or more molecules. For each of these cluster, we have selected one  
302 representative structure and additionally we have found the maximum common substructure  
303 (MCS) using the FMCS algorithm implemented in RDKit. We discovered that for all compounds

304 in the cluster with the representative structure A in Figure 7, the fold-changes were predicted with  
305 low errors ( $AE < 1.0$ ). The compounds in this cluster have certain substructures with HIV  
306 inhibitors, such as a sulfonamide group, a bis-THF alcohol moiety, and a benzodioxole group [46].  
307 The only structural difference in this cluster of compounds was observed on the side chain  
308 connecting to the phenoxy group. Our model, on the other hand, did not perform well for another  
309 cluster of compounds represented by structure B in Figure 7. Despite the fact that the MCS for  
310 three compounds in this cluster were similar to the preceding cluster, represented by structure A,  
311 there were subtle differences that caused compounds to be in distinct clusters. For these, the  
312 cyclohexyl hydroxy or cyclopentyl hydroxy group was attached to the N of the sulfonamide group.  
313 Furthermore, the varying side group of the phenoxy group in the first cluster was shorter in the  
314 second cluster since there was only phenyl group. Compounds having structure C are represented  
315 in another cluster, as seen in Figure 7. These compounds had a high resemblance to the IDV (see  
316 Figure 4 for a 2D representation of the IDV), and the fold-change was predicted with minimal  
317 errors ( $AE < 1.0$ ). These compounds, like the IDV, have substructure groups such as  
318 piperazinecarboxamide, indenol derivative, and phenyl group. However, the compounds in this  
319 cluster have different attachment groups connected to piperazine ring instead of pyridine group in  
320 the IDV. We have also discovered that for the compound where the fold change estimation error  
321 above the threshold ( $AE \geq 1.0$ ), the exact value was 1.01, indicating that it is negligible. It should  
322 be noted, however, that this compound contains a Fluorine substituent, which is known to cause a  
323 significant increase in the inhibitory activity of compounds [47] and it may not be easily learnt  
324 using our model. This chemical similarity analysis revealed that our model can predict the fold  
325 change for similar compounds with low error, despite the fact that some of the external set  
326 molecules based on our descriptors were not similar (or in close proximity in the PCA plot in  
327 Figure 7) to internal set molecules.

328

## 329 **Discussions**

330 This paper presents a machine learning approach for predicting fold-change values using HIV-1  
331 protease inhibitor and isolate characteristics. The filtered PhenoSense assay results made  
332 accessible in the Stanford HIV drug resistance database have been used training and  
333 testing machine learning models. Seven of the eight inhibitors have been used to train drug-isolate-  
334 fold change-based feed-forward artificial neural networks, with the remaining one serving as test

335 data (LVO). In this context, the LVO procedure produces an objective testing approach for  
336 determining the learning capacity of models from the descriptors of the inhibitors. Both inhibitors  
337 and isolates have been encoded using binary mappings, which have been shown to be  
338 computationally effective. Because of their acknowledged advantages in molecular machine  
339 learning models, the Morgan fingerprints have been exploited as binary mappings of protease  
340 inhibitors [41-43]. An efficient ensemble process has been proposed and verified through various  
341 quantitative experiments to handle the overfitting trouble.

342 The most significant contribution of this research is the construction of drug-isolate-fold change  
343 (DIF)-based ANN models, as opposed to the widely studied isolate-fold change (IF)-based models  
344 [29-40]. Because the IF models do not take the molecular fingerprints as input, they are insensitive  
345 to molecular structure. This study shows the possibility of achieving such a generalized model by  
346 feeding models with adequate data from various PIs in the presence of isolates. With the use of the  
347 LVO procedure throughout our investigation, the current DIF-based models have been shown to  
348 be capable of predicting the drug resistance profiles of unknown inhibitors. Even though the  
349 Stanford HIV database only has eight available inhibitors, having many isolates for each inhibitor  
350 has contributed to the learning process, and reasonable predictions have been found in the  
351 regression performance of remaining inhibitors.

352 The prediction of drug resistance tendencies for each PI pair is an unavoidable expectation from  
353 our DIF-based ANN models. Our generalized models can predict resistance trends with high 2D  
354 correlation scores, as demonstrated here. The DIF-based models have provided satisfactory  
355 accuracy, sensitivity, specificity, and MCC values by creating classification problems from the  
356 tendency relations of each PI pair. The DIF-based ANN model utilizes valuable information from  
357 the Morgan fingerprints to predict the fold change values of hidden inhibitors, according to our  
358 all-quantitative observations.

359 We have shown that our ANN model can categorize resistant and susceptible strains as well as  
360 rank inhibitors based on resistance profiles for an external dataset. The external dataset is designed  
361 in such a way that the unique molecules are comparable enough to any of the primary eight PI and  
362 there is no bit loss in the reduction procedure of the Morgan fingerprints from 512 to 234  
363 dimensions. Thus, whenever a molecule satisfies these conditions, our DIF-based model has ability  
364 to compare this molecule with existing PIs in terms of their resistance scores.

365 Instead of building independent separate models for each inhibitor, this study offers a fresh  
366 viewpoint on the field by incorporating inhibitor characteristics on the input side of machine  
367 learning models. The most obvious drawback of our model is the dearth of protease inhibitors with  
368 sufficient genotype-phenotype information. Nevertheless, our encouraging findings have  
369 demonstrated that including genotype-phenotype information of novel protease inhibitors will help  
370 build more generic drug-isolate-fold change-based machine learning models. Additionally,  
371 feeding the DIF-based models with data from many conventional and nonconventional inhibitors  
372 may result in a unified model for forecasting drug resistance tendencies for any PI pair in the  
373 presence of known genotypes. The drug development process for evolvable diseases, such as HIV,  
374 bacterial infections, and cancer should be fundamentally different from diseases such as blood-  
375 pressure regulators. A drug needs to be effective and stay effective through the test of evolution.  
376 Predicting resistance potentials for drugs is becoming a necessity.

377

### 378 **Conclusions**

379 This study has revealed the advantages of developing DIF-based models to predict drug resistance  
380 profiles. Instead of IF-based models, the current approach has allowed us to investigate a new  
381 model that can predict the drug resistance tendencies of PI pairs. Even with only eight PIs  
382 available, internal and external test results show that the DIF-based model takes significant  
383 information from inhibitor descriptors and leads to satisfactory regression performance. As a  
384 result, after finishing this study, it is highlighted on the research agenda to train ANN models with  
385 more inhibitors by expanding the existing dataset. In this context, it will be feasible to track the  
386 drug resistance profiles of any novel protease inhibitor, and it is strongly believed that these  
387 insightful forecasts will be a right direction for moving forward.

388

### 389 **Author Contributions**

390 Conceptualization: [Huseyin Tunc, Enes Seyfullah Kotil]; Methodology: [Huseyin Tunc, Enes  
391 Seyfullah Kotil, Berna Dogan, Busra Nur Darendeli Kiraz]; Formal analysis and investigation:  
392 [Huseyin Tunc]; Writing - original draft preparation: [Huseyin Tunc]; Writing - review and  
393 editing: [Huseyin Tunc, Murat Sari, Serdar Durdagi, Enes Seyfullah Kotil, Berna Dogan]; Funding  
394 acquisition: [Enes Seyfullah Kotil]; Resources: [Enes Seyfullah Kotil]; Supervision: [Murat Sari,  
395 Serdar Durdagi, Enes Seyfullah Kotil].

396

397 **Data and Software Availability**

398 All data and necessary codes are deposited to:

399 [https://github.com/tchsyn/hivdrugisolatefoldchange\\_model](https://github.com/tchsyn/hivdrugisolatefoldchange_model)400 <https://doi.org/10.5281/zenodo.7527918>

401

402 **References**

- 403 1. Sharp P, Hahn BH (2011) Origins of HIV and the AIDS Pandemic. Cold Spring Harb  
404 Perspect 1:006841. <https://doi.org/10.1101/cshperspect.a006841>
- 405 2. Das K, Arnold E HIV-1 (2013) Reverse transcriptase and antiviral drug resistance (Part 1  
406 of 2). *Curr Opin Virol* 3(2):111–118. <https://doi.org/10.1016/j.coviro.2013.03.014>
- 407 3. Lu DY, Wu HY, Yarla, NS, Xu B, Ding J, Lu TR (2018) HAART in HIV/AIDS Treatments:  
408 Future Trends. *Infect Disord Drug Targets* 18(1):15-22. <https://doi.org/10.2174/1871526517666170505122800>
- 410 4. Jespersen NA, Axelsen F, Dollerup J, Nørgaard M, Larsen CS (2021) The burden of non-  
411 communicable diseases and mortality in people living with HIV (PLHIV) in the pre-, early-  
412 and late-HAART era. *HIV Medicine*. <https://doi.org/10.1111/hiv.13077>
- 413 5. Palmisano L, Vella S (2011) A brief history of antiretroviral therapy of HIV infection:  
414 success and challenges. *Ann Ist Super Sanità* 47(1):44-48.  
415 [https://doi.org/10.4415/ANN\\_11\\_01\\_10](https://doi.org/10.4415/ANN_11_01_10)
- 416 6. World Health Organization. Global HIV/AIDS response: epidemic update and health sector  
417 progress towards universal access: progress report.  
418 <https://apps.who.int/iris/handle/10665/44787>
- 419 7. Günthard HF, Calvez V, Paredes R, Pillay D, Shafer RW, Wensing AM, Jacobsen DM,  
420 Richma DD (2019) Human Immunodeficiency Virus Drug Resistance: 2018  
421 Recommendations of the International Antiviral Society–USA Panel. *Clin Infect Dis*  
422 68(2):177–187. <https://doi.org/10.1093/cid/ciy463>
- 423 8. Kuritzkes DR (2011) Drug resistance in HIV-1. *Curr Opin Virol* 1(6):582-589.  
424 <https://doi.org/10.1016/j.coviro.2011.10.020>
- 425 9. Oroz M, Begovac J, Planinic A, Rokic F, Lunar MM, Zorec TM, Beluzić R, Korać P,  
426 Vugrek O, Poljak M, Lepej SZ (2019) Analysis of HIV-1 diversity, primary drug resistance

- 427 and transmission networks in Croatia. *Sci Rep* 9:17307. [https://doi.org/10.1038/s41598-](https://doi.org/10.1038/s41598-019-53520-8)  
428 019-53520-8
- 429 10. Lagnese M, Daar ES (2008) Antiretroviral regimens for treatment-experienced patients  
430 with HIV-1 infection. *Expert Opin Pharmacother* 9:5:687-700. [https://doi.org/](https://doi.org/10.1517/14656566.9.5.687)  
431 10.1517/14656566.9.5.687
- 432 11. Cihlar T, He GX, Liu X, Chen JM, Hatada M, Swaminathan S, McDermott MJ, Yang ZY,  
433 Mulato AS, Chen X, Leavitt SA, Stray KM, Lee WA (2006) Suppression of HIV-1 protease  
434 inhibitor resistance by phosphonate-mediated solvent anchoring. *J Mol Biol* 363:635–647.  
435 [https://doi.org/ 10.1016/j.jmb.2006.07.073](https://doi.org/10.1016/j.jmb.2006.07.073)
- 436 12. Stranix BR, Sauve G, Bouzide A, Cote A, Sevigny G, Yelle J (2003) Lysine sulfonamides  
437 as novel HIV-protease inhibitors: Optimization of the Nepsilon-acyl-phenyl spacer. *Bioorg*  
438 *Med Chem Lett* 13:289–4292. [https://doi.org/ 10.1016/j.bmcl.2003.09.058](https://doi.org/10.1016/j.bmcl.2003.09.058)
- 439 13. Nakatani S, Hidaka K, Ami E, Nakahara K, Sato A, Nguyen JT, Hamada Y, Hori Y, Ohnishi  
440 N, Nagai A, Kimura T, Hayashi Y, Kiso Y (2008) Combination of non-natural D-amino  
441 acid derivatives and allophenylnorstatine-dimethylthiopropine scaffold in HIV protease  
442 inhibitors have high efficacy in mutant HIV. *J Med Chem* 51:2992–3004.  
443 <https://doi.org/10.1021/jm701555p>
- 444 14. Koh Y, Das D, Leschenko S, Nakata H, Ogata-Aoki H, Amano M, Nakayama M, Ghosh  
445 AK, Mitsuya H (2009) GRL-02031, a novel nonpeptidic protease inhibitor (PI) containing  
446 a stereochemically defined fused cyclopentanyltetrahydrofuran potent against multi-PI-  
447 resistant human immunodeficiency virus type 1 in vitro. *Antimicrob Agents Chemother*  
448 53(3):997-1006. <https://doi.org/10.1128/AAC.00689-08>
- 449 15. Koh Y, Nakata H, Maeda K, Ogata H, Bilcer G, Devasamudram T, Kincaid JF, Boross P,  
450 Wang YF, Tie Y, Volarath P, Gaddis L, Harrison RW, Weber IT, Ghosh AK, Mitsuya H  
451 (2003) Novel bis-tetrahydrofuranylurethane-containing nonpeptidic protease inhibitor (PI)  
452 UIC-94017 (TMC114) with potent activity against multi-PI-resistant human  
453 immunodeficiency virus in vitro. *Antimicrob Agents Chemother* 47(10):3123-9.  
454 [https://doi.org/ 10.1128/AAC.47.10.3123-3129.2003](https://doi.org/10.1128/AAC.47.10.3123-3129.2003)
- 455 16. Zhang S, Kaplan AH, Tropsha A (2008) HIV-1 protease function and structure studies with  
456 the simplicial neighborhood analysis of protein packing method. *Proteins* 73(3): 742–753.  
457 [https://doi.org/ 10.1002/prot.22094](https://doi.org/10.1002/prot.22094)

- 458 17. World Health Organization. Updated recommendations on first-line and second-line  
459 antiretroviral regimens and post-exposure prophylaxis and recommendations on early infant  
460 diagnosis of HIV, <https://www.who.int/publications/i/item/WHO-CDS-HIV-18.51>.
- 461 18. Rosenbloom DIS, Hill AL, Rabi SA (2012) Antiretroviral dynamics determines HIV  
462 evolution and predicts therapy outcome. *Nat Med* 18(9):1378-1386. [https://doi.org/](https://doi.org/10.1038/nm.2892)  
463 10.1038/nm.2892
- 464 19. Jilek BL, Zarr M, Sampah ME, Rabi SA, Bullen CK, Lai J, Shen L, Siliciano RF (2011) A  
465 quantitative basis for antiretroviral therapy for HIV-1 infection. *Nat Med* 18(3):446-452.  
466 [https://doi.org/ 10.1038/nm.2649](https://doi.org/10.1038/nm.2649)
- 467 20. Xing H, Ruan Y, Li J, Shang H, Zhong P, Wang X, Liao L, Li H, Zhang M, Xue Y, Wang  
468 Z, Su B, Liu W, Dong Y, Ma Y, Li H, Qin G, Chen L, Pan X, Chen X, Peng G, Fu J, Chen  
469 RY, Kang L, Shao Y (2013) HIV Drug Resistance and Its Impact on Antiretroviral Therapy  
470 in Chinese HIV-Infected Patients. *PLoS ONE* 8(2): e54917.  
471 <https://doi.org/10.1371/journal.pone.0054917>
- 472 21. Lima VD, Gill VS, Yip B, Hogg RS, Montaner JS, Harrigan PR (2008) Increased Resilience  
473 to the Development of Drug Resistance with Modern Boosted Protease Inhibitor-Based  
474 Highly Active Antiretroviral Therapy. *J Infect Dis* 198(1):51–58. [https://doi.org/](https://doi.org/10.1086/588675)  
475 10.1086/588675
- 476 22. Wei Y, Li J, Chen Z, Wang F, Huang W, Hong Z, Lin J (2015) Multistage virtual screening  
477 and identification of novel HIV-1 protease inhibitors by integrating SVM, shape,  
478 pharmacophore and docking methods. *Eur J Med Chem* 101:409–418.  
479 <https://doi.org/10.1016/j.ejmech.2015.06.05>
- 480 23. Yu X, Weber IT, Harrison RW (2014) Prediction of HIV drug resistance from genotype  
481 with encoded three-dimensional protein structure. *BMC Genom* 15:1-13.  
482 <https://doi.org/10.1186/1471-2164-15-S5-S1>
- 483 24. Hosseini A, Alibés A, Noguera-Julian M (2016) Computational Prediction of HIV-1  
484 Resistance to Protease Inhibitors. *J Chem Inf Model* 56(5): 915–923. [https://doi.org/](https://doi.org/10.1021/acs.jcim.5b00667)  
485 10.1021/acs.jcim.5b00667
- 486 25. Talbot A, Grant P, Taylor J, Baril JG, Liu TF, Charest H, Brenner B, Roger M, Shafer R,  
487 Cantin R, Zolopa A (2010) Predicting tipranavir and darunavir resistance using genotypic,  
488 phenotypic, and virtual phenotypic resistance patterns: an independent cohort analysis of

- 489 clinical isolates highly resistant to all other protease inhibitors. *Antimicrob Agents*  
490 *Chemother* 54:2473-2479. <https://doi.org/10.1128/AAC.00096-10>
- 491 26. Obermeier M, Pironti A, Berg T, Braun P, Daumer M, Eberle J, Ehret R, Kaiser R,  
492 Kleinkauf N, Korn K, Kücherer C, Müller H, Noah C, Stürmer M, Thielen A, Wolf E,  
493 Walter H (2012) HIVGRADE: a publicly available, rules-based drug resistance  
494 interpretation algorithm integrating bioinformatic knowledge. *Intervirology* 55:102-107.  
495 <https://doi.org/10.1159/000331999>
- 496 27. Van Laethem K, De Luca A, Antinori A, Cingolani A, Perno CF (2002) A genotypic drug  
497 resistance interpretation algorithm that significantly predicts therapy response in HIV-1-  
498 infected patients. *Antivir Ther* 7:123–129. <https://doi.org/10.1177/135965350200700206>
- 499 28. Meynard JL, Vray M, Morand-Joubert L, Race E, Descamps D, Peytavin G, Matheron S,  
500 Lamotte C, Guiramand S, Costagliola D, Brun-Vezinet F, Clavel F, Girard PM (2002)  
501 Phenotypic or genotypic resistance testing for choosing antiretroviral therapy after treatment  
502 failure: a randomized trial. *AIDS* 16:727–736. [https://doi.org/10.1097/00002030-](https://doi.org/10.1097/00002030-200203290-00008)  
503 [200203290-00008](https://doi.org/10.1097/00002030-200203290-00008)
- 504 29. Amamuddy OS, Bishop NT, Bishop OT (2017) Improving fold resistance prediction of  
505 HIV-1 against protease and reverse transcriptase inhibitors using artificial neural networks.  
506 *BMC Bioinform* 18:369-376. <https://doi.org/10.1186/s12859-017-1782-x>
- 507 30. Amamuddy OS, Bishop NT, Bishop OT (2018) Characterizing early drug resistance-related  
508 events using geometric ensembles from HIV protease dynamics. *Sci Rep* 8:17938.  
509 <https://doi.org/10.1038/s41598-018-36041-8>
- 510 31. Wang D, Larder B (2003) Enhanced Prediction of Lopinavir Resistance from Genotype by  
511 Use of Artificial Neural Networks. *J Infect Dis* 88(5):653–660. [https://doi.org/](https://doi.org/10.1086/377453)  
512 [10.1086/377453](https://doi.org/10.1086/377453)
- 513 32. Drăghici S, Potter RR (2002) Predicting HIV drug resistance with neural networks.  
514 *Bioinformatics* 19(1):98-107. <https://doi.org/10.1093/bioinformatics/19.1.98>
- 515 33. Kjaer J, Høj L, Fox Z, Lundgren J (2008) Prediction of phenotypic susceptibility to  
516 antiretroviral drugs using physiochemical properties of the primary enzymatic structure  
517 combined with artificial neural networks. *HIV Medicine* 9:642-652. [https://doi.org/](https://doi.org/10.1111/j.1468-1293.2008.00612.x)  
518 [10.1111/j.1468-1293.2008.00612.x](https://doi.org/10.1111/j.1468-1293.2008.00612.x)

- 519 34. Steiner MC, Gibson KM, Crandall KA (2020) Drug Resistance Prediction Using Deep  
520 Learning Techniques on HIV-1 Sequence Data. *Viruses* 12:560. [https://doi.org/](https://doi.org/10.3390/v12050560)  
521 10.3390/v12050560
- 522 35. Wang D, Larder B, Revell A, Montaner J, Harrigan R, De Wolf F, Lange J, Wegner S, Ruiz  
523 L, Pérez-Eliás MJ, Emery S, Gatell J, Monforte AD, Torti C, Zazzi M, Lane C (2009) A  
524 Comparison of three computational modelling methods for the prediction of virological  
525 response to combination HIV therapy. *Artif Intell Med* 47:63-74. [https://doi.org/](https://doi.org/10.1016/j.artmed.2009.05.002)  
526 10.1016/j.artmed.2009.05.002
- 527 36. Shen CH, Yu X, Harrison RW, Weber IT (2016) Automated prediction of HIV drug  
528 resistance from genotype data. *BMC Bioinform* 17:278-285. [https://doi.org/](https://doi.org/10.1186/s12859-016-1114-6)  
529 10.1186/s12859-016-1114-6
- 530 37. Shah D, Freas C, Weber IT, Harrison RW (2020) Evolution of drug resistance in HIV  
531 protease. *BMC Bioinform* 21:497-512. <https://doi.org/10.1186/s12859-020-03825-7>
- 532 38. Tarasova O, Biziukova N, Kireev D, Lagunin A, Ivanov S, Filimonov D, Poroikov V (2020)  
533 A Computational Approach for the Prediction of Treatment History and the Effectiveness  
534 or Failure of Antiretroviral Therapy. *Int J Mol Sci* 21(3):748.  
535 <https://doi.org/10.3390/ijms21030748>
- 536 39. Tarasova O, Biziukova N, Filimonov D, Poroikov V (2018) A Computational Approach for  
537 the Prediction of HIV Resistance Based on Amino Acid and Nucleotide Descriptors.  
538 *Molecules* 23(11):2751. <https://doi.org/10.3390/molecules23112751>
- 539 40. Ota R, So K, Tsuda M, Higuchi Y, Yamashita F (2021) Prediction of HIV drug resistance  
540 based on the 3D protein structure: Proposal of molecular field mapping. *PLoS ONE*  
541 16(8):e0255693. <https://doi.org/10.1371/journal.pone.0255693>
- 542 41. Cai Q, Yuan R, He J, Menglong L, Yanzhi G (2021) Predicting HIV drug resistance using  
543 weighted machine learning method at target protein sequence-level. *Mol Divers*, 25:1541–  
544 1551. <https://doi.org/10.1007/s11030-021-10262-y>
- 545 42. Beerenwinkel N, Daumer M, Oette M, Korn K, Hoffmann D, Kaiser R, Lengauer T, Selbig  
546 J, Walter H (2003) Geno2pheno: estimating phenotypic drug resistance from HIV-1  
547 genotypes. *Nucleic Acids Res* 31:3850-3855. <https://doi.org/10.1093/nar/gkg575>
- 548 43. Beerenwinkel N, Schmidt B, Walter H, Kaiser R, Lengauer T, Hoffmann D, Korn K, Selbig  
549 J (2002) Diversity and complexity of HIV-1 drug resistance: a bioinformatics approach to

- 550 predicting phenotype from genotype. PNAS 99:8271-8276.  
551 <https://doi.org/10.1073/pnas.112177799>
- 552 44. Pawar SD, Freas C, Weber IT, Harrison RW (2018) Analysis of drug resistance in HIV  
553 protease. BMC Bioinform 19:362-368. <https://doi.org/10.1186/s12859-018-2331-y>
- 554 45. Rhee SY, Taylor J, Fessel WJ (2010) HIV-1 Protease Mutations and Protease Inhibitor  
555 Cross-Resistance. Antimicrob Agents Chemother 54(10):4253–4261. <https://doi.org/10.1128/AAC.00574-10>
- 556
- 557 46. Sevenich A, Liu GQ, Arduengo III AJ, Gupton BF, Opatz T. (2017) Asymmetric One-Pot  
558 Synthesis of (3 R, 3a S, 6a R)-Hexahydrofuro [2, 3-b] furan-3-ol: A Key Component of  
559 Current HIV Protease Inhibitors. J Org Chem Jan 82(2):1218-23.  
560 <https://doi.org/10.1021/acs.joc.6b02588>
- 561 47. Amano M, Yedidi RS, Salcedo-Gómez PM, Hayashi H, Hasegawa K, Martyr CD, Ghosh  
562 AK, Mitsuya H. (2022) Fluorine Modifications Contribute to Potent Antiviral Activity  
563 against Highly Drug-Resistant HIV-1 and Favorable Blood-Brain Barrier Penetration  
564 Property of Novel Central Nervous System-Targeting HIV-1 Protease Inhibitors In Vitro.  
565 Antimicrob Agents Chemother 66(2):e01715-21. <https://doi.org/10.1128/aac.01715-21>

**Table 1** (on next page)

Predictive performance of DIF-based ANN models.

Mean square error (MSE) and  $R^2$  values of the DIF-based ANN models for predicting the logarithmic fold change values of eight PIs are presented. Drug-isolate-fold change models are constructed as a general neural network model taking drug fingerprints and mutation information as inputs. For each row, the corresponding drug has not been included in the training process. The test set performance of each model has been evaluated with respect to the excluded drugs. 100\*50 simulations with random weights have been done, and 100 neural network models that yield minimum MSE for interior test set among 50 trials are obtained. The final neural network model is achieved by taking the mean of 100 models. Abbreviations: ATV, atazanavir; DRV, darunavir; FPV, fosamprenavir; IDV, indinavir; LPV, lopinavir; NFV, nelfinavir; SQV, saquinavir; TPV, tipranavir.

- 1 **Table 1.** Mean square error (MSE) and  $R^2$  values of the DIF-based ANN models for predicting  
 2 the logarithmic fold change values of 8 PIs are presented<sup>b</sup>.

ARVs <sup>a</sup>	$R^2$		MSE	
	Whole dataset	Test set	Whole dataset	Test set
ATV	0.865	0.778	0.087	0.166
DRV	0.857	0.736	0.092	0.227
FPV	0.849	0.738	0.097	0.160
IDV	0.861	0.811	0.090	0.131
LPV	0.852	0.822	0.096	0.188
NFV	0.845	0.757	0.101	0.215
SQV	0.833	0.731	0.109	0.283
TPV	0.821	0.359	0.116	0.560

- 3 <sup>a</sup> Abbreviations: ATV, atazanavir; DRV, darunavir; FPV, fosamprenavir; IDV, indinavir; LPV, lopinavir; NFV,  
 4 nelfinavir; SQV, saquinavir; TPV, tipranavir.

- 5 <sup>b</sup> Drug-isolate-fold change models are constructed as a general neural network model taking drug fingerprints and  
 6 mutation information as inputs. For each row, the corresponding drug has not been included in the training process.  
 7 The test set performance of each model has been evaluated with respect to the excluded drugs.  $100 \times 50$  simulations  
 8 with random weights have been done, and 100 neural network models that yield minimum MSE for interior test set  
 9 among 50 trials are obtained. The final neural network model is achieved by taking the mean of 100 models.

10

11

**Table 2** (on next page)

Accuracy, sensitivity, specificity and MCC values of the DIF-based ANN models for predicting the drug resistance tendencies for each couple of ARVs.

Accuracy, sensitivity and specificity values represent the rate of true predictions, true positive rate and true negative rate, respectively. The common genotype data is used for each PI pair by eliminating the observations satisfying  $|\log(A)-\log(B)| \leq \log 2$  where A and B are the fold change values of drugs A and B for a specified genotype.

- 1 **Table 2.** Accuracy, sensitivity, specificity and MCC values of the DIF-based ANN models for
- 2 predicting the drug resistance tendencies for each couple of ARVs<sup>a</sup>.

ARVs		ATV	DRV	FPV	IDV	LPV	NFV	SQV	TPV
ATV	Accuracy	-	0.970 (224/231)	0.932 (438/470)	0.923 (264/286)	0.913 (303/332)	0.948 (361/381)	0.896 (301/336)	0.983 (404/411)
	Sensitivity	-	0.500 (7/14)	0.772 (78/101)	0.850 (85/100)	0.978 (178/182)	0.986 (291/295)	0.720 (90/125)	0.000 (0/6)
	Specificity	-	1.000 (217/217)	0.976 (360/369)	0.962 (179/186)	0.833 (125/150)	0.814 (70/86)	1.000 (211/211)	0.998 (404/405)
	MCC	-	0.696	0.791	0.829	0.828	0.856	0.786	0.000
DRV	Accuracy	0.970 (224/231)	-	0.968 (184/190)	0.917 (222/242)	0.960 (215/224)	0.976 (321/329)	0.936 (206/220)	0.897 (156/174)
	Sensitivity	1.000 (217/217)	-	0.972 (172/177)	0.966 (198/205)	0.982 (214/218)	1.000 (308/308)	0.972 (173/178)	0.714 (40/56)
	Specificity	0.500 (7/14)	-	0.923 (12/13)	0.649 (24/37)	0.167 (1/6)	0.619 (13/21)	0.786 (33/42)	0.983 (116/118)
	MCC	0.696	-	0.792	0.662	0.162	0.777	0.788	0.761
FPV	Accuracy	0.932 (438/470)	0.968 (184/190)	-	0.936 (677/723)	0.952 (511/537)	0.964 (878/911)	0.930 (705/758)	0.932 (369/396)
	Sensitivity	0.976 (360/369)	0.923 (12/13)	-	0.993 (552/556)	0.996 (465/467)	0.996 (817/820)	0.975 (502/515)	0.511 (24/47)
	Specificity	0.772 (78/101)	0.972 (172/177)	-	0.749 (125/167)	0.657 (46/70)	0.670 (61/91)	0.835 (203/243)	0.989 (345/349)
	MCC	0.791	0.792	-	0.816	0.771	0.782	0.838	0.630
IDV	Accuracy	0.923 (264/286)	0.917 (222/242)	0.936 (677/723)	-	0.952 (399/419)	0.952 (498/523)	0.929 (562/605)	0.957 (404/422)
	Sensitivity	0.962 (179/186)	0.649 (24/37)	0.749 (125/167)	-	0.989 (270/273)	0.994 (468/471)	0.874 (221/253)	0.280 (7/25)
	Specificity	0.850 (85/100)	0.966 (198/205)	0.993 (552/556)	-	0.884 (129/146)	0.577 (30/52)	0.969 (341/352)	1.000 (397/397)
	MCC	0.829	0.662	0.816	-	0.895	0.702	0.854	0.518
LPV	Accuracy	0.913 (303/332)	0.960 (215/224)	0.952 (511/537)	0.952 (399/419)	-	0.944 (526/557)	0.929 (509/548)	0.982 (429/437)
	Sensitivity	0.833 (125/150)	0.167 (1/6)	0.657 (46/70)	0.884 (129/146)	-	0.979 (375/383)	0.836 (173/207)	0.632 (12/19)
	Specificity	0.978 (178/182)	0.982 (214/218)	0.996 (465/467)	0.989 (270/273)	-	0.868 (151/174)	0.985 (336/341)	0.998 (417/418)
	MCC	0.828	0.162	0.770	0.895	-	0.869	0.850	0.755
NFV	Accuracy	0.948 (361/381)	0.976 (321/329)	0.964 (878/911)	0.952 (498/523)	0.944 (526/557)	-	0.935 (735/786)	0.966 (477/494)
	Sensitivity	0.814 (70/86)	0.619 (13/21)	0.670 (61/91)	0.577 (30/52)	0.868 (151/174)	-	0.451 (41/91)	0.188 (3/16)
	Specificity	0.986 (291/295)	1.000 (308/308)	0.996 (817/820)	0.994 (468/471)	0.979 (375/383)	-	0.999 (694/695)	0.992 (474/478)
	MCC	0.846	0.777	0.782	0.702	0.869	-	0.639	0.268
SQV	Accuracy	0.896 (301/336)	0.936 (206/220)	0.930 (705/758)	0.929 (562/605)	0.929 (509/548)	0.935 (735/786)	-	0.898 (359/400)
	Sensitivity	1.000 (211/211)	0.786 (33/42)	0.835 (203/243)	0.969 (341/352)	0.985 (336/341)	0.999 (694/695)	-	0.146 (7/48)
	Specificity	0.720	0.972	0.975	0.874	0.836	0.451	-	1.000

		(90/125)	(173/178)	(502/515)	(221/253)	(173/207)	(41/91)		(352/352)
	MCC	<b>0.786</b>	<b>0.788</b>	<b>0.838</b>	<b>0.854</b>	<b>0.850</b>	<b>0.639</b>	-	<b>0.361</b>
TPV	Accuracy	<b>0.983</b> (404/411)	<b>0.897</b> (156/174)	<b>0.932</b> (369/396)	<b>0.957</b> (404/422)	<b>0.982</b> (429/437)	<b>0.966</b> (477/494)	<b>0.898</b> (359/400)	-
	Sensitivity	<b>0.998</b> (404/405)	<b>0.983</b> (116/118)	<b>0.989</b> (345/349)	<b>1.000</b> (397/397)	<b>0.998</b> (417/418)	<b>0.992</b> (474/478)	<b>1.000</b> (352/352)	-
	Specificity	<b>0.000</b> (0/6)	<b>0.714</b> (40/56)	<b>0.511</b> (24/47)	<b>0.280</b> (7/25)	<b>0.632</b> (12/19)	<b>0.188</b> (3/16)	<b>0.146</b> (7/48)	-
	MCC	<b>0.000</b>	<b>0.761</b>	<b>0.630</b>	<b>0.518</b>	<b>0.755</b>	<b>0.268</b>	<b>0.361</b>	-

3 <sup>a</sup> Accuracy, sensitivity and specificity values represent the rate of true predictions, true positive  
4 rate and true negative rate, respectively. The common genotype data is used for each PI pair by  
5 eliminating the observations satisfying  $|\log(A) - \log(B)| \leq \log 2$  where  $A$  and  $B$  are the fold  
6 change values of drugs  $A$  and  $B$  for a specified genotype.

7

**Table 3**(on next page)

Classification performance of the ANN model on the external test data.

In resistance classification procedure, the ANN model is used to classify the genotypes as drug resistant (Fold Change  $\geq 3$ ) and susceptible (Fold Change  $< 3$ ) for each external test data. On the other hand, for ranking classification procedure, the ANN ranks the drugs for a given genotype in terms of their logarithmic fold change values.

1 **Table 3.** Classification performance of the ANN model on the external test data. In resistance  
2 classification procedure, the ANN model is used to classify the genotypes as drug resistant (  
3 *Fold Change*  $\geq 3$ ) and susceptible (*Fold Change*  $< 3$ ) for each external test data. On the other  
4 hand, for ranking classification procedure, the ANN ranks the drugs for a given genotype in terms  
5 of their logarithmic fold change values.

Model / Metric	Accuracy	Sensitivity	Specificity	MCC	AUC
Resistance Classification	0.678	0.536	0.935	0.468	0.843
Ranking Classification	0.749	0.767	0.730	0.497	0.819

6

7

# Figure 1

Data versus the predicted fold change values from DIF-based ANN models.

DIF-based ANN regression models are constructed with the LVO testing methodology. For each figure, the fold-change results are estimated by an ANN model, which is trained with the remaining data of the seven PIs. The  $R^2$  values correspond to the square of the linear correlation coefficient of the data and prediction.

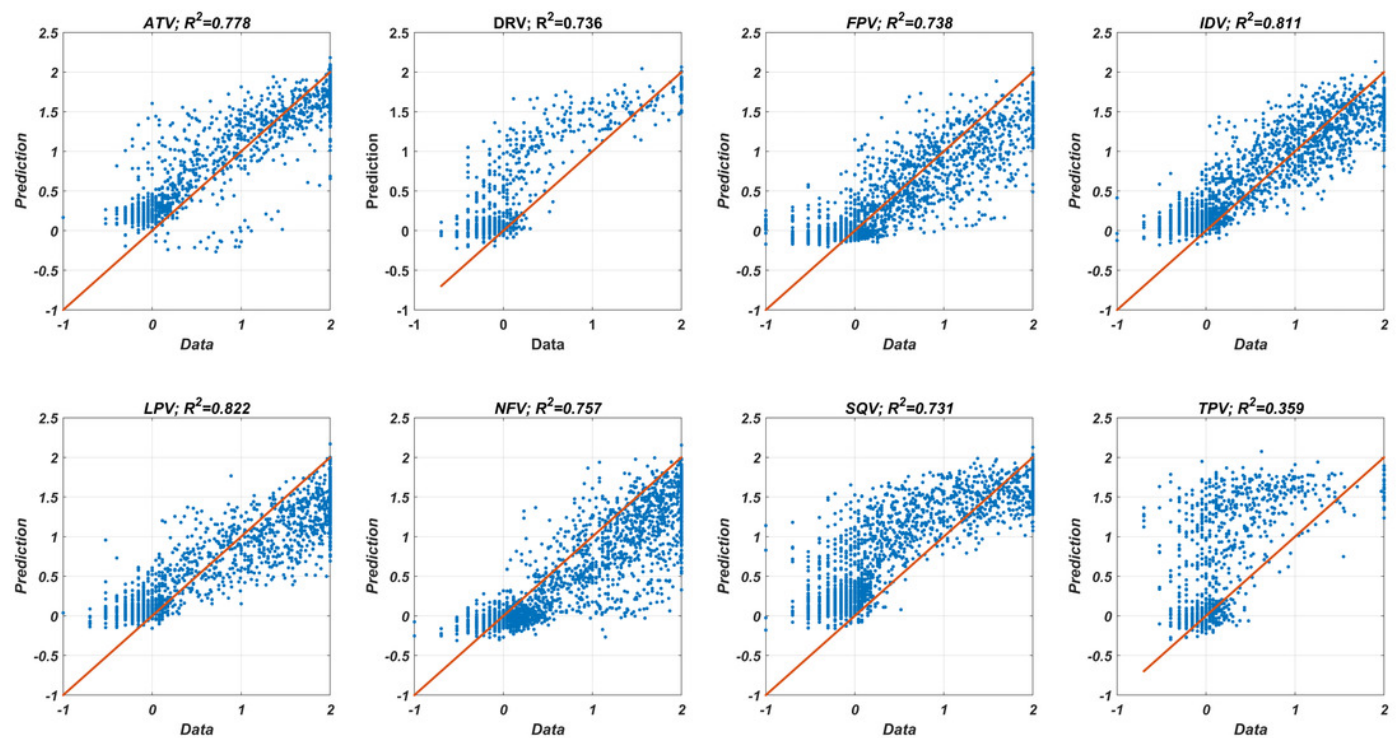


## Figure 2

Prediction of the fold-change tendencies with the DIF-based ANN model for each PI pair.

The common isolate data of each PI pair and the corresponding DIF-based ANN model predictions are illustrated with 2D correlation coefficients. For each PI, the prediction is constructed using the DIF-based ANN model, which is trained with the remaining seven PI data. The illustrations show the tendencies of the drug resistances for each PI pair for common genotypes.

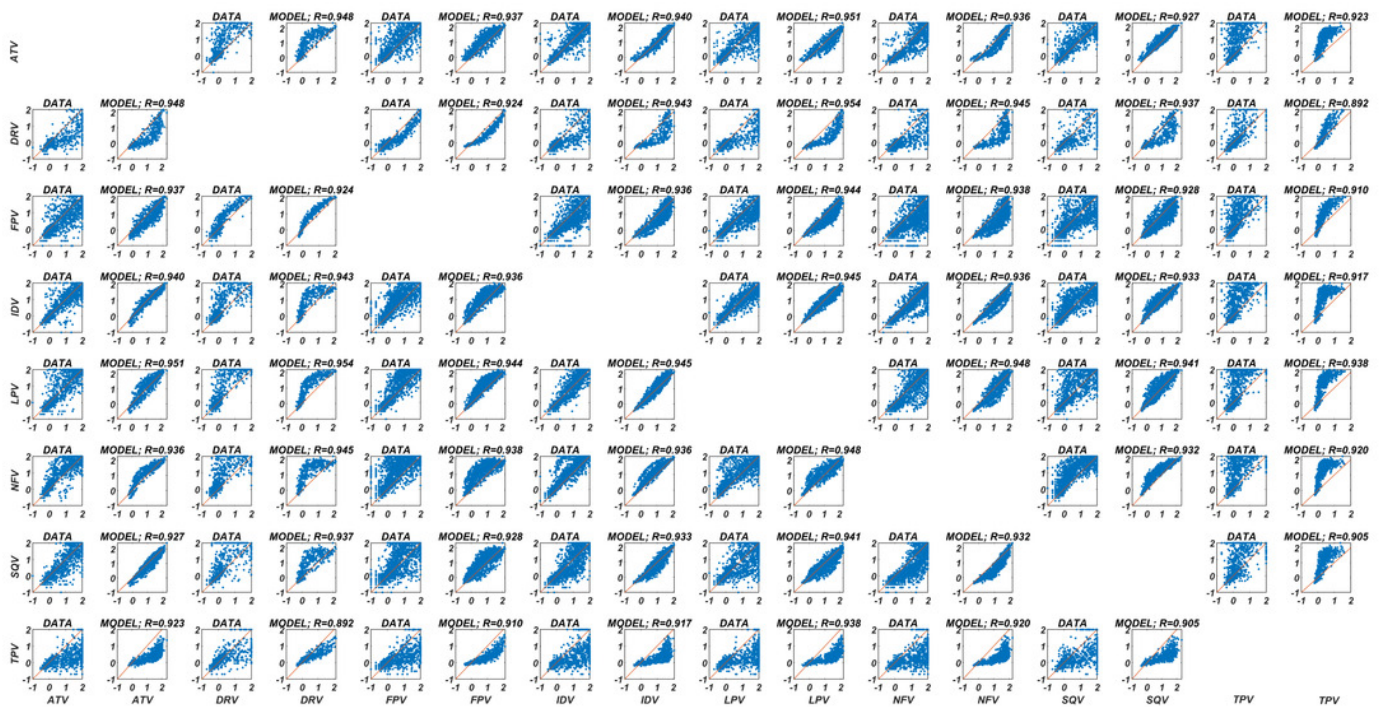


## Figure 3

### Classification performances of the DIF-based ANN models

The DIF-based ANN classification models are constructed with the LVO methodology. For each PI, the classification of resistant and non-resistant isolates is estimated by an ANN model trained with the remaining data of the seven PI. The AUC values correspond to the area under the ROC curves, and the accuracy is evaluated with the true estimation rate.

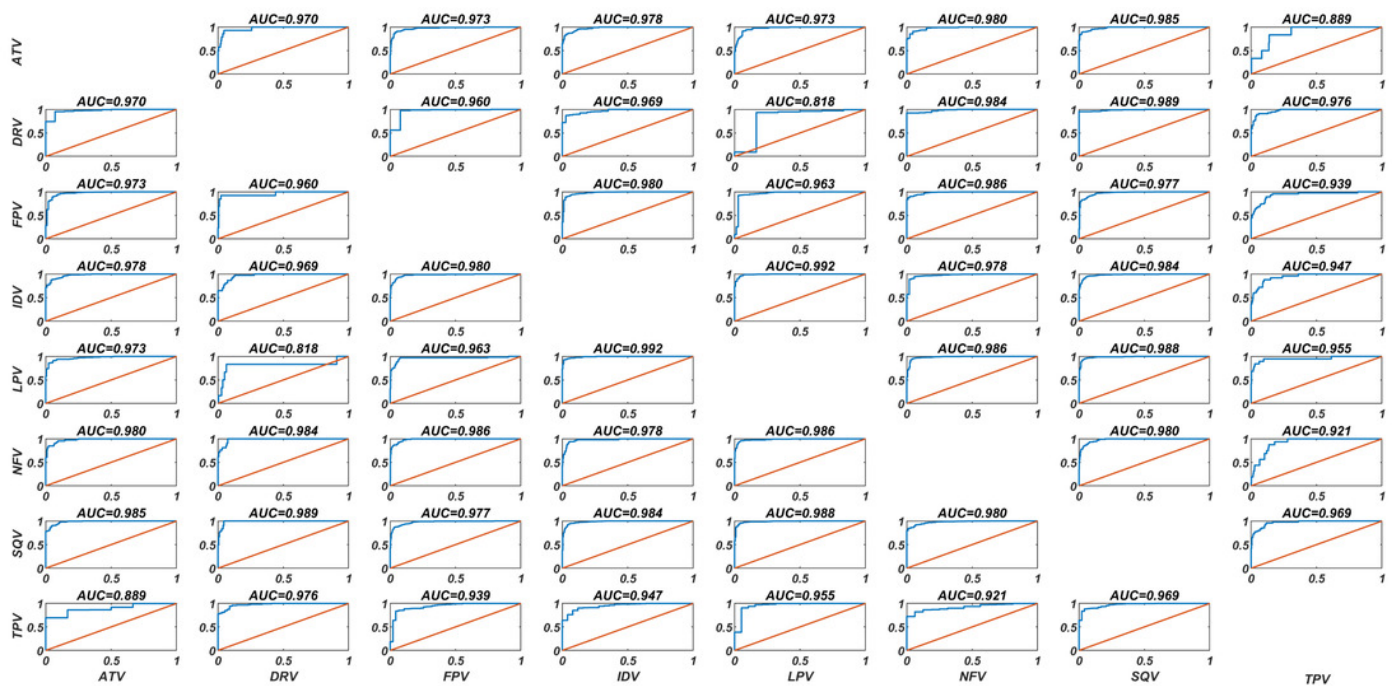
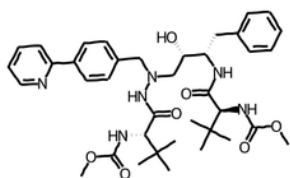
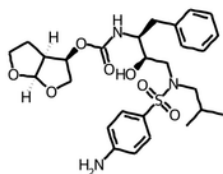


## Figure 4

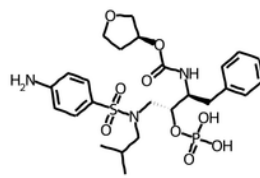
Chemical structures of eight PIs utilized in the DIF-based ANN model training.



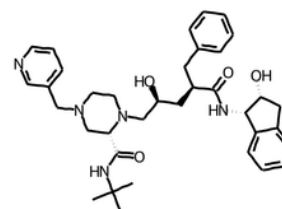
ATV



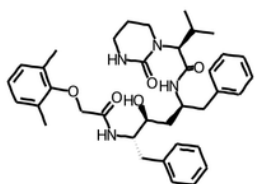
DRV



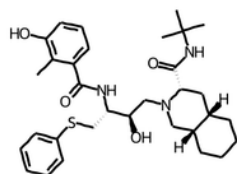
FPV



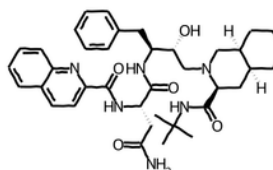
IDV



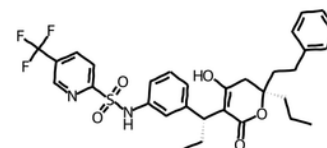
LPV



NFV



SQV

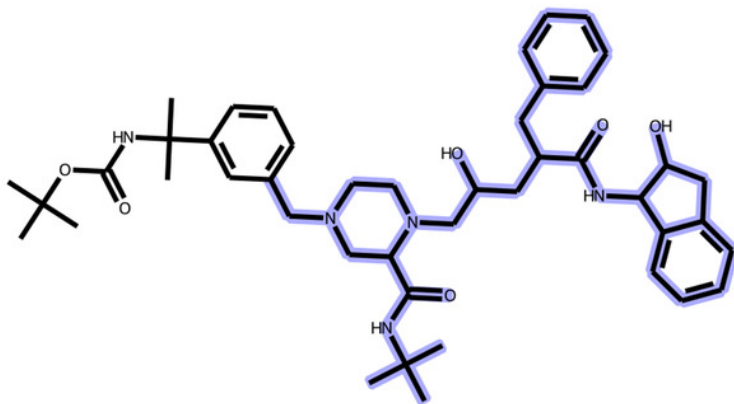


TPV

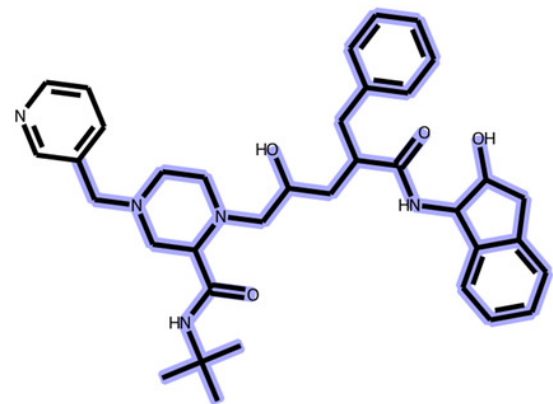
## Figure 5

Resistance classification for two compounds having similar structures.

A ranking classification example for two compounds that have similar structures with different resistance profiles for the same strain (L10I, L19Q, K20R, E35D, M36I, S37N, M46I, I50V, I54V, I62V, L63P, A71V, V82A, L90M, E28K, K32E, V35I, T39T, E40DV, M41L, K43E, Y181Y).



**ChEMBL ID** = CHEMBL405134  
**Experimental Fold-change** = 436.52  
**Predicted Fold-change** = 2.82



**ChEMBL ID** = CHEMBL115  
**Experimental Fold-change** = 1.15  
**Predicted Fold-change** = 1.74

## Figure 6

The ROCs corresponding to resistance and ranking classifications for the test data.

The DIF-based ANN model has been used to (A) classify the resistance and susceptible strains (B) classify the rankings of 853 pair of resistance scores, for various molecules existing our external data. The AUC ratings associated with the ROC curves measure how threshold probabilities affect FPR-TPR pairs in classification tasks.

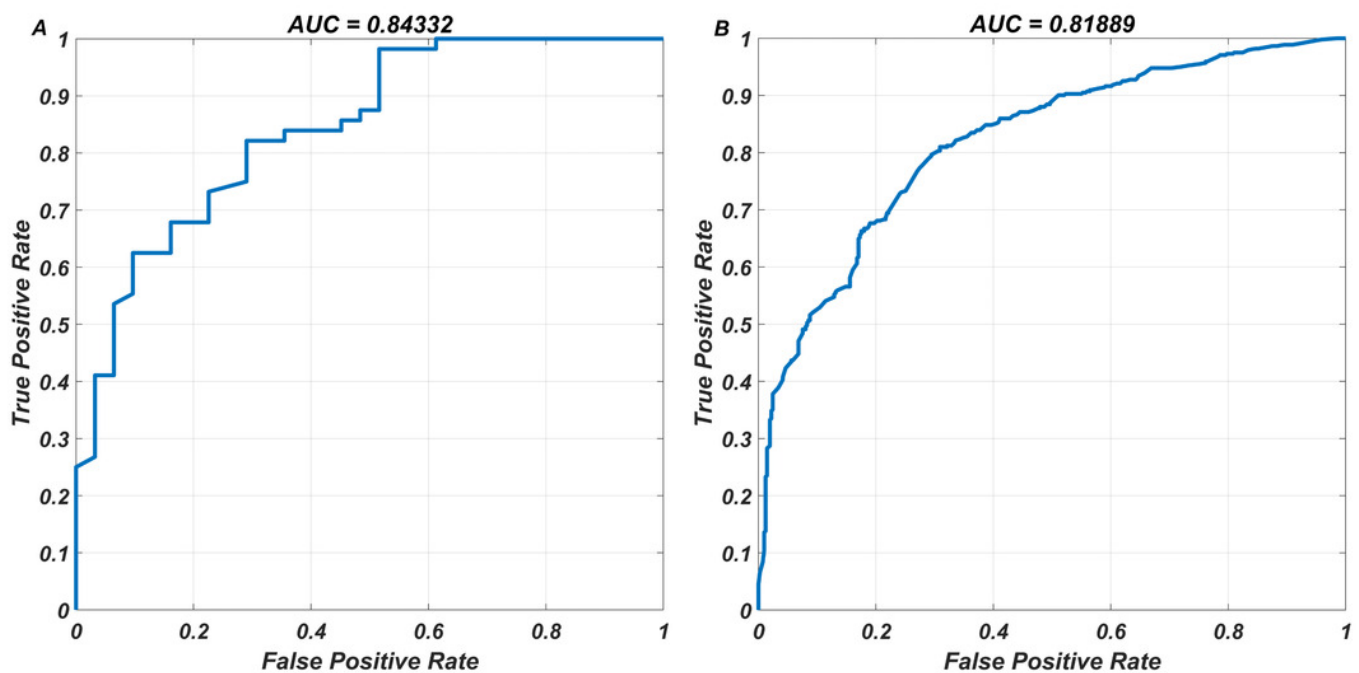


## Figure 7

PCA plot for external set molecules obtained using the unique characteristic 234 bits fingerprint descriptors.

PCA plot for external set molecules produced with the unique 234-bit fingerprint descriptors. The absolute error (AE) for fold change prediction using the model is calculated for each molecule. Molecules are classified with respect to corresponding AE values (AE=1 is selected as threshold). The data points in black are for the existing eight PIs, which have their names indicated. As demonstrated, example structures from clusters are exhibited and designated A, B, and C. In the 2D depiction, the most prevalent substructures in the same clusters have been highlighted in dark blue.

